Copenhagen '12

Y012

Creating Virtual Sources Inside an Unknown Medium from Reflection Data - A New Approach to Internal Multiple Elimination

K. Wapenaar* (Delft University of Technology), J. Thorbecke (Delft University of Technology), J. van der Neut (Delft University of Technology), F. Broggini (Colorado School of Mines) & R. Snieder (Colorado School of Mines)

SUMMARY

It has recently been shown that the response to a virtual source in the subsurface can be derived from reflection data at the surface and an estimate of the direct arrivals between the virtual source and the surface. Hence, unlike for seismic interferometry, no receivers are needed inside the medium. This new method recovers the complete wavefield of a virtual source, including all internal multiple scattering. Because no actual receivers are needed in the medium, the virtual source can be placed anywhere in the subsurface. With some additional processing steps (decomposition and multidimensional deconvolution) it is possible to obtain a redatumed reflection response at any depth level in the subsurface, from which all the overburden effects are eliminated. By applying standard migration between these depth levels, a true amplitude image of the subsurface can be obtained, free from ghosts due to internal multiples. The method is non-recursive and therefore does not suffer from error propagation. Moreover, the internal multiples are eliminated by deconvolution, hence no adaptive prediction and subtraction is required.

Introduction

We discuss a new approach to creating the response to a virtual source inside an unknown medium that goes beyond seismic interferometry and that can be used as a basis for internal multiple elimination. Broggini *et al.* (2011, 2012) show that, given the reflection response of a 1D layered medium, it is possible to obtain the response to a virtual source inside the medium, without the need to know the medium parameters. The method consists of an iterative scheme, akin to earlier work of Rose (2002). Interestingly, the response retrieved by this new method contains all scattering effects of the layered medium. Note that, in order to obtain the same virtual-source response by seismic interferometry, one would need a receiver at the position of the virtual source inside the medium, and real sources at the top and bottom of the medium. Hence, the advantage of the new 1D approach over 1D seismic interferometry is that no receivers are needed inside the medium and that the medium needs to be illuminated from one side only.

Last year we made a first step towards generalizing this idea to the 3D situation (Wapenaar *et al.*, 2011). Using physical arguments we proposed an iterative scheme that transforms the reflection response of a 3D medium into the response to a virtual source inside the 3D medium. Whereas controlled-source seismic interferometry (Schuster *et al.*, 2004; Bakulin and Calvert, 2006) requires receivers in the subsurface (Figure 1a), the proposed scheme requires reflection data at the surface (Figure 1b) and an estimate of the direct arrivals between the virtual source and the acquisition surface. The method recovers the complete wavefield of a virtual source, including internal multiple scattering, without needing any information about the location and strength of the interfaces. Similar as in seismic interferometry, the virtual source is closer to the reservoir. However, unlike for interferometry, no actual receivers are needed inside the medium. Moreover, by repeated application, virtual sources and virtual receivers can be obtained anywhere inside the medium (Figure 1c). We show in this paper that from the reconstructed wavefields inside the medium it is possible to obtain improved images, free of ghosts caused by internal multiple scattering. The proposed method requires a background model for the primary arrivals, but the internal multiple prediction and elimination is data-driven. The method is non-recursive and therefore does not suffer from error propagation. The internal multiples are eliminated by deconvolution, hence no adaptive prediction and subtraction is required.

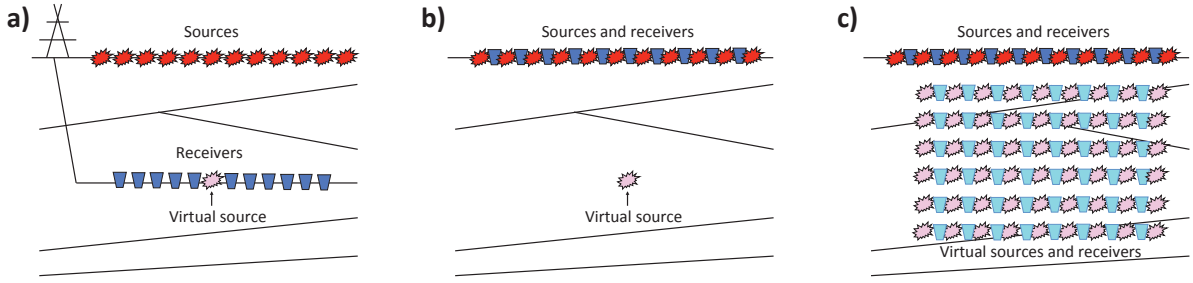

Figure 1: *(a) Controlled-source seismic interferometry creates virtual sources in the subsurface at the position of receivers in a borehole (Schuster et al., 2004; Bakulin and Calvert, 2006). (b) Data-driven wavefield reconstruction (Broggini* et al.*, 2011; Wapenaar* et al.*, 2011) also creates virtual sources in the subsurface, but uses sources and receivers at the surface. (c) Repeated application gives virtual sources and virtual receivers throughout the medium, leading to improved images, free of ghosts caused by internal multiple scattering.*

Initiating the iterative process

We discuss an iterative scheme that creates the response to a virtual source in the subsurface from reflection data at the surface (for details see Wapenaar *et al.*, 2011, 2012). The scheme is initiated with an estimate of the direct arrivals between the virtual source at $\mathbf{x}_{VS} = (x_{VS}, z_{VS})$ and the surface. These direct arrivals are reversed in time, which turns the upgoing field at the surface $z = 0$ into a downgoing field $p_0^+(\mathbf{x}, t)$, see Figure 2a (the red curves will be discussed in the next section). The field $p_0^+(\mathbf{x}, t)$ is used as the initial downgoing field at $z = 0$. It is convolved with the reflection response of the medium, according to

$$p_0^-(\mathbf{x}_R, t) = \int_{-\infty}^{\infty} \left[R(\mathbf{x}_R, \mathbf{x}, t) * p_0^+(\mathbf{x}, t)\right]_{z=0} \mathrm{d}x, \tag{1}$$

for $z_R = 0$. Here $R(\mathbf{x}_R, \mathbf{x}, t)$ is the measured reflection response, after surface-related multiple elimination and deconvolution for the source wavelet. The result of this convolution is the upgoing wave field $p_0^-(\mathbf{x}, t)$

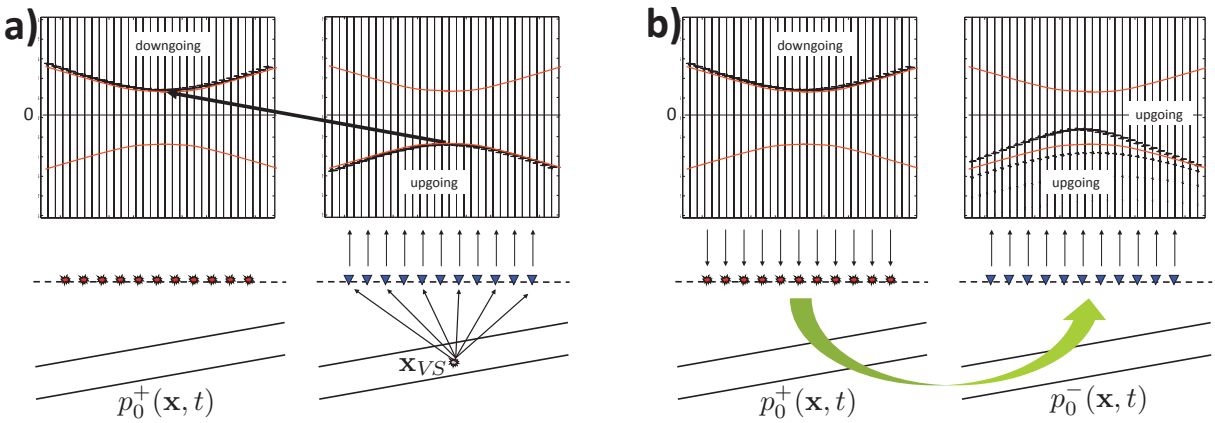

Figure 2: *Initiating the iterative process. (a) An estimate of the direct field between the virtual source and the surface is reversed in time, giving the initial downgoing field* $p_0^+(\mathbf{x},t)$. *(b) The initial downgoing field* $p_0^+(\mathbf{x},t)$ *is convolved with the reflection response of the medium, giving the upgoing field* $p_0^-(\mathbf{x},t)$.

at the surface, see Figure 2b. For this example we have evaluated the integral by the method of stationary phase, which explains why no aperture effects are present in Figure 2b. In practice, equation (1) will be evaluated numerically, which will introduce artifacts related to the finite aperture.

The iterative process

We define two traveltime curves, indicated by the red solid lines. The lower curve is taken just before the direct arrival of Figure 2a and the upper curve is defined as the time-reversal of the lower curve, hence, it comes directly after the initial incident field $p_0^+(\mathbf{x},t)$. We define a window function $w(\mathbf{x},t)$ that equals 1 between these red curves and 0 elsewhere. We discuss an iterative scheme, which has the aim to modify the incident field in such a way that, within the time window, the incident field is equal to minus the time-reversed reflection response. We will motivate this peculiar condition in the next section. To achieve this goal, the kth iteration is defined as follows

$$p_k^+(\mathbf{x},t) = p_0^+(\mathbf{x},t) - w(\mathbf{x},t)p_{k-1}^-(\mathbf{x},-t), \tag{2}$$

$$p_k^-(\mathbf{x}_R,t) = \int_{-\infty}^{\infty}\left[R(\mathbf{x}_R,\mathbf{x},t) * p_k^+(\mathbf{x},t)\right]_{z=0}\mathrm{d}x, \tag{3}$$

for $\mathbf{x}$ and $\mathbf{x}_R$ at $z=0$. The reflection response $p_0^-(\mathbf{x},t)$ is shown in Figure 2b. Only the response of the first reflector (the first event) falls within the time window. We subtract the time-reversal of this event from $p_0^+(\mathbf{x},t)$, which gives, according to equation (2) for $k=1$, the modified incident wave field $p_1^+(\mathbf{x},t)$, see Figure 3a. Using equation (3) we evaluate the reflection response $p_1^-(\mathbf{x},t)$ to this modified incident wave field, which is also shown in Figure 3a. Note that, within the time window, $p_1^-(\mathbf{x},t)$ is identical to $p_0^-(\mathbf{x},t)$, hence, further iterations will not cause any changes. Already after one iteration we have achieved the desired situation mentioned at the beginning of this section. This is a consequence of analyzing the simple configuration with two interfaces only. For more complex configurations more iterations will be required.

Creating the virtual-source response

After finalizing the iterative process, we define $p(\mathbf{x},t)$ as the superposition of the final incident and reflected wave fields at $z=0$. Because, for this example, iteration $k=1$ was the final iteration, we have $p(\mathbf{x},t) = p_1^+(\mathbf{x},t) + p_1^-(\mathbf{x},t)$. This total field is shown in Figure 3b (left frame). Within the time window this field is antisymmetric in time (this was the design criterion for the iterative scheme). Hence, if we superpose the total field and its time-reversed version, i.e., $p_{\mathrm{sym}}(\mathbf{x},t) = p(\mathbf{x},t) + p(\mathbf{x},-t)$, all events within the time window will cancel each other, whereas outside the time window this superposition will be symmetric, see Figure 3b (right frame). Note that, because we consider a lossless medium, $p_{\mathrm{sym}}(\mathbf{x},t)$ obeys the wave equation. Since time-reversal changes the propagation direction, it follows that the causal part is upward propagating at $z=0$ and the acausal part is downward propagating at $z=0$. The first arrival of the causal part of $p_{\mathrm{sym}}(\mathbf{x},t)$ in Figure 3b corresponds with the direct arrival of the response to the virtual source at $\mathbf{x}_{VS}$ (Figure 2a). Given this last observation, combined with the fact that the causal part is upward propagating at $z=0$ and that the total field obeys the wave equation and is

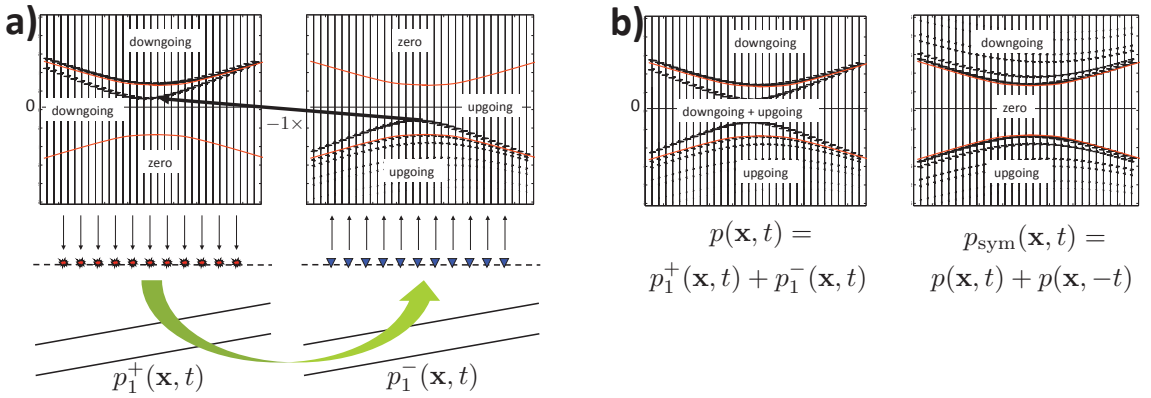

Figure 3: *(a) The iterative process. The event(s) of the upgoing field between the red curves is (are) reversed in time and subtracted from the initial downgoing field. The modified downgoing field* $p_k^+(\mathbf{x},t)$ *(here* $k=1$*) is convolved with the reflection response of the medium, giving the modified upgoing field* $p_k^-(\mathbf{x},t)$*. (b) Left frame: Superposition of downgoing and upgoing field. Right frame: superposition of total field and its time-reversal. This is interpreted as* $G(\mathbf{x},\mathbf{x}_{VS},t) + G(\mathbf{x},\mathbf{x}_{VS},-t)$*.*

symmetric, it is plausible that $p_{\mathrm{sym}}(\mathbf{x},t)$ is proportional to $G(\mathbf{x},\mathbf{x}_{VS},t) + G(\mathbf{x},\mathbf{x}_{VS},-t)$ (where G stands for the Green's function in the real medium). This argumentation holds for more general situations, but it has been checked explicitly with the stationary-phase method for the response in Figure 3b (right frame) (Wapenaar *et al.*, 2012). Figure 4a shows once more the direct arrival of Figure 2a, with which we initiated the iterative process, and the causal part of $p_{\mathrm{sym}}(\mathbf{x},t)$ (Figure 3b, right frame), which is interpreted as the Green's function $G(\mathbf{x},\mathbf{x}_{VS},t)$. Note that the direct arrival in this retrieved Green's function comes from our initial estimate, whereas the internal multiples come entirely from the measured reflection response.

Decomposition

The Green's function $G(\mathbf{x},\mathbf{x}_{VS},t)$ is the response to the virtual source at $\mathbf{x}_{VS}$. In Figure 4a it is clearly seen that this source radiates upward as well as downward propagating fields. The latter arrive at the surface after having been reflected at the interface below the source. We now discuss how the source can be decomposed into an upward and a downward radiating source. To this end we first repeat the iterative process, but we replace the minus sign in equation (2) and Figure 3a by a plus sign. When this iterative process is finished, we define again the total field as $p(\mathbf{x},t) = p_1^+(\mathbf{x},t) + p_1^-(\mathbf{x},t)$, of which the part within the time window is now symmetric in time (instead of antisymmetric). Hence, by evaluating $p_{\mathrm{asym}}(\mathbf{x},t) = p(\mathbf{x},t) - p(\mathbf{x},-t)$, all events within the time window will again cancel each other (like in Figure 3b), whereas outside the time window this field is antisymmetric. The new created virtual source is therefore also antisymmetric (like a dipole). If we subtract this new response from our retrieved monopole response, i.e., if we evaluate $\frac{1}{2}\{p_{\mathrm{sym}}(\mathbf{x},t) - p_{\mathrm{asym}}(\mathbf{x},t)\}$ and take the causal part, we obtain the response to an upward radiating virtual source, whereas the causal part of the superposition $\frac{1}{2}\{p_{\mathrm{sym}}(\mathbf{x},t) + p_{\mathrm{asym}}(\mathbf{x},t)\}$ yields the response to a downward radiating virtual source, see Figure 4b.

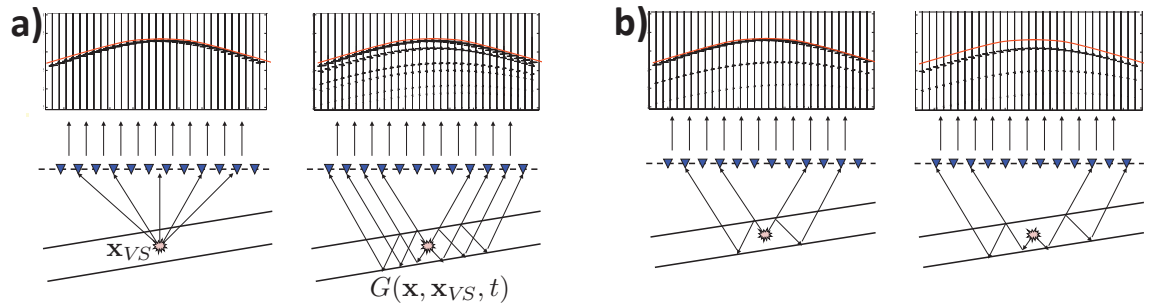

Figure 4: *(a) Comparison of the direct arrivals (Figure 2a) and the retrieved Green's function* $G(\mathbf{x},\mathbf{x}_{VS},t)$ *(the causal part of Figure 3b). (b) Decomposition of the virtual source into an upward and downward radiating virtual source.*

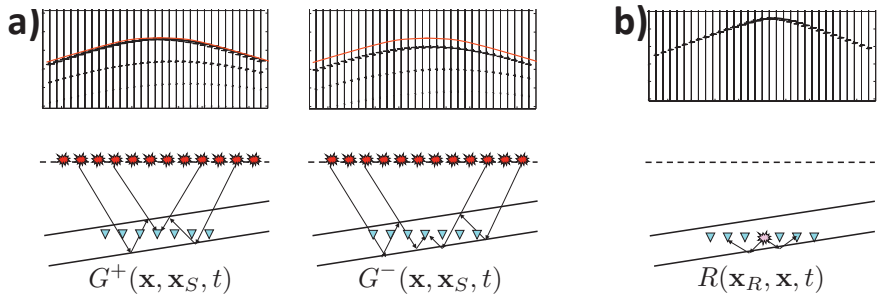

Figure 5: *(a) As in Figure 4b, but after applying source-receiver reciprocity. (b) Result of applying multidimensional deconvolution to the responses of (a). This is the redatumed reflection response, free of overburden effects. Repeating this for all depth levels leads to a multiple-free image of the subsurface.*

Imaging without internal multiple ghosts

Using source-receiver reciprocity, a virtual-source response observed by receivers at the surface is equal to the response to sources at the surface, observed by a virtual receiver in the subsurface. Hence, the decomposed responses of Figure 4b are, after applying source-receiver reciprocity, interpreted as the downward and upward propagating fields at a virtual receiver in the subsurface, due to sources at the surface, i.e., as $G^+(\mathbf{x}, \mathbf{x}_S, t)$ and $G^-(\mathbf{x}, \mathbf{x}_S, t)$, respectively, with $\mathbf{x}$ at the virtual-source depth z_{VS}, see Figure 5a. For a range of virtual receivers at z_{VS}, these responses are related via

$$G^-(\mathbf{x}_R, \mathbf{x}_S, t) = \int_{-\infty}^{\infty} \left[R(\mathbf{x}_R, \mathbf{x}, t) * G^+(\mathbf{x}, \mathbf{x}_S, t)\right]_{z=z_{VS}} \mathrm{d}x, \tag{4}$$

for $\mathbf{x}_R$ at z_{VS}. Here $R(\mathbf{x}_R, \mathbf{x}, t)$ is the reflection response at the virtual-source depth z_{VS}, for the situation of a homogeneous overburden. It can be resolved from $G^+(\mathbf{x}, \mathbf{x}_S, t)$ and $G^-(\mathbf{x}, \mathbf{x}_S, t)$ by multidimensional deconvolution (MDD), similar as in seismic interferometry by MDD. Figure 5b shows the MDD result (again without artifacts because for this example we evaluated it by the method of stationary phase). It can be seen as the redatumed reflection response from which all the overburden effects have been eliminated. By repeating the entire process for many depth levels, as indicated in Figure 1c, and applying standard migration in between these depth levels, a true amplitude image of the subsurface can be obtained, free from ghosts due to internal multiples. The advantages and disadvantages of the proposed approach with respect to other internal multiple elimination schemes (Weglein *et al.*, 1997; Berkhout and Verschuur, 1997; Jakubowicz, 1998; etc.) need further investigation.

Conclusions

For a simple configuration we have shown that it is possible to create the response to a virtual source in the subsurface from the reflection response at the surface and an estimate of the direct arrivals. Following the physical arguments in the section "Creating the virtual-source response", it is plausible that this procedure will also work in more complex environments. Nevertheless, the method will also have its limitations. The effects of a finite acquisition aperture, errors in the direct arrivals, triplications, head waves, diving waves, fine-layering etc. need further investigation. A first numerical test by one of us (FB) with a variable-velocity syncline model shows promising results. For those configurations for which it is possible to create virtual sources from reflection data, the method can be used as a basis to image the subsurface without internal multiple ghosts. Because the proposed method is non-recursive, the data-driven prediction of internal multiples will not suffer from error propagation. Because the internal multiples are eliminated by deconvolution, no adaptive prediction and subtraction is required. Last, but not least, the internal multiples contribute to the restoration of the amplitudes of the primary reflections.

References

Bakulin, A., and Calvert, R. [2006] *Geophysics* 71(4), SI139–SI150.
Berkhout, A. J., and Verschuur, D. J. [1997] *Geophysics* 62, 1586–1595.
Broggini, F., Snieder, R., and Wapenaar, K. [2011] *pp 3845–3850 of: SEG, Expanded Abstracts.*
Broggini, F., Snieder, R., and Wapenaar, K. [2012] *Geophysics* (submitted).
Jakubowicz, H. [1998] *pp 1527–1530 of: SEG, Expanded Abstracts.*
Rose, J. H. [2002] *Inverse Problems* 18, 1923–1934.
Schuster, G. T., Yu, J., Sheng, J., and Rickett, J. [2004] *Geophysical Journal International* 157, 838–852.
Wapenaar, K., Broggini, F., and Snieder, R. [2011] *pp 3788–3792 of: SEG, Expanded Abstracts.*
Wapenaar, K., Broggini, F., and Snieder, R. [2012] *Geophysical Journal International* (submitted).
Weglein, A. B., Gasparotto, F. A., Carvalho, P. M., and Stolt, R. H. [1997] *Geophysics* 62(6), 1975–1989.